# Glucose-dependent activation, activity, and deactivation of beta cell networks in acute mouse pancreas tissue slices

Jurij Dolenšek [1,2], Maša Skelin Klemen[1], Marko Gosak[1,2], Lidija Križančić-Bombek[1], Viljem Pohorec[1], Marjan Slak Rupnik [1,3, 4, *], Andraž Stožer[1*]

[1] Institute of Physiology, Faculty of Medicine, University of Maribor, Taborska 8, SI-2000 Maribor, Slovenia

[2] Faculty of Natural Sciences and Mathematics, University of Maribor, Koroška cesta 160, SI-2000 Maribor, Slovenia

[3] Center for Physiology and Pharmacology, Medical University of Vienna, Schwarzspanierstraße 17A, 1090 Vienna, Austria

[4]Alma Mater Europaea – European Center Maribor, Slovenska ulica 17, 2000 Maribor

* corresponding authors

## Abstract

Glucose progressively stimulates insulin release over a wide range of concentrations. However, the nutrient coding underlying activation, activity, and deactivation of beta cells affecting insulin release remains only partially described. Experimental data indicate that nutrient sensing in coupled beta cells in islets is predominantly a collective trait, overriding to a large extent functional differences between cells. However, some degree of heterogeneity between coupled beta cells may play important roles. To further elucidate glucose-dependent modalities in coupled beta cells, the degree of functional heterogeneity, and uncover the emergent collective operations, we combined acute mouse pancreas tissue slices with functional multicellular calcium imaging. We recorded beta cell calcium responses from threshold (7 mM) to supraphysiological (16 mM) glucose concentrations with high spatial and temporal resolution. This enabled the analysis of both classical physiological parameters and complex network parameters, as well as their comparison at the level of individual cells. The activation profile displayed two major glucose concentration-dependent features, shortening of delays to initial activation, and shortening of delays until half activation with increasing glucose concentration. Inversely, during deactivation both delays to initial deactivation and until half deactivation were progressively longer with increasing glucose concentration. The plateau activity with fast calcium oscillations expressed two types of glucose-dependence. Physiological concentrations mostly affected the frequency of oscillations, whereas supraphysiological concentrations progressively prolonged the duration of oscillations. Most of the measured functional network parameters also showed clear glucose-dependence. In conclusion, we propose novel understanding for glucose-dependent coding properties in beta cell networks, and its deciphering may have repercussions for our understanding of the normal physiology of glucose homeostasis as well as of disturbances of metabolic homeostasis, such as diabetes mellitus.

## 1. Introduction

Glucose is one of the main insulin secretagogues in beta cells. After entering beta cells through GLUT (Skelin Klemen, Dolenšek et al. 2017) or other transporters (Rorsman & Ashcroft, Physiol Rev 2018), glucose initiates cellular processes leading to transient activation of beta cells, followed by subsequent periodic oscillatory changes in membrane potential and intracellular calcium concentration ($[Ca^{2+}]_{IC}$), as well as insulin secretion (Ashcroft and Rorsman 1989). The calcium ion is a central secondary messenger, coupling stimulation with secretion not only for nutrient secretagogues but also for other neurohormonal stimuli. Glucose-dependent oscillatory $[Ca^{2+}]_{IC}$ changes have been reported *in vivo* in an exteriorized pancreas and in islets transplanted into the anterior chamber of the eye, *in situ* in acute pancreas tissue slices, as well as *in vitro* in enzymatically isolated and cultured islets (Bergsten, Grapengiesser et al. 1994, Bertuzzi, Davalli et al. 1999, Fernandez and Valdeolmillos 2000, Benninger, Zhang et al. 2008, Benninger, Hutchens et al. 2014). $[Ca^{2+}]_{IC}$ oscillations are the triggering signal for fusion of insulin-containing vesicles with the plasma membrane, thus driving a periodical release of insulin. Importantly, the extent of insulin secretion is further regulated by various additional signals in both $[Ca^{2+}]_{IC}$-dependent and $[Ca^{2+}]_{IC}$-independent manner (Henquin 2011). Regardless of the pathways taken to induce and regulate insulin secretion, $[Ca^{2+}]_{IC}$ dynamics remains a convenient proxy for assessment of both more proximal and distal events in the stimulus-secretion coupling cascade. Compared with measurements of membrane potential changes and insulin secretion, functional multicellular calcium imaging typically offers a better combination of the number of cells that can be analyzed simultaneously, spatial and temporal resolution, and the recording time.

A substantial number of previous studies attempted to address the glucose dependency of beta cells stimulation, however a complete characterization of the complex relationship with stimulus intensity remains elusive. Both *ex vivo* (Ashcroft, Bassett et al. 1972, Gao, Drews et al. 1990, Detimary, Jonas et al. 1995, Henquin, Nenquin et al. 2006, Benninger, Head et al. 2011, Low, Mitchell et al. 2013) and *in vivo* experiments (Henquin, Nenquin et al. 2006) show that insulin secretion progressively increases over a wide range of physiological and supraphysiological glucose concentrations. In dissociated beta cells in culture, glucose thresholds for single beta cell activation differed greatly among individual beta cells from low to supraphysiological glucose concentrations (Jonkers and Henquin 2001, Benninger, Head et al. 2011), suggesting that such heterogeneity in sensitivity to glucose could be the underlying mechanism for a progressive recruitment of additional beta cells to a secretory response . However, beta cells in an intact islets function in a coupled, collective way and such coupling significantly narrows the concentration range over which the whole islet activates, with the half maximal effective concentration of glucose ($EC_{50}$) at about 7 mM (Dean and Matthews 1970, Benninger, Head et al. 2011). It is therefore likely that additional mechanisms contribute to the insulin release above the physiological glucose range. Among these, different sources of amplification, e.g., hormonal, neuronal, and metabolic, could also contribute to the elevated average calcium concentrations driving increased insulin release and corresponding to progressively higher glucose concentrations in uncoupled (Jonkers and Henquin 2001) as well as in coupled beta cells (Gylfe 1988, Antunes, Salgado et al. 2000, Henquin, Nenquin et al. 2006). Along these lines, the frequency and duration of intracellular calcium oscillations as

well as bursts of electrical activity change with the progressive increase in glucose concentration (Meissner and Schmelz 1974, Cook and Ikeuchi 1989, Henquin 1992, Antunes, Salgado et al. 2000, Lebreton, Pirog et al. 2015). And the cumulative increase in intracellular calcium has been found to exert its main effect through increasing the number of fusion events of granules containing insulin (Low, Mitchell et al. 2013) [add Masa Ceca 2011]. This was also recently corroborated by mathematical modelling of experimental data demonstrating that both mobilization and priming of insulin granules were the main factors determining concentration-dependent insulin secretion (Pedersen, Tagliavini et al. 2019). Alternatively, the effects observed at supraphysiological glucose concentrations could also be due mechanisms that are not set into motion at lower concentrations of glucose. It is important to emphasize that although the physiological range of glucose dependence of insulin release has been known for decades, most often, the experiments are still being performed at supraphysiological (typically >10 mM) glucose concentrations.

Applying functional multicellular calcium imaging by confocal scanning microscopy in acute pancreas tissue slices (Stožer, Dolenšek et al. 2013, Stožer, Gosak et al. 2013, Markovic, Stozer et al. 2015), we previously demonstrated that beta cells within an islet typically display a biphasic $[Ca^{2+}]_{IC}$ response. From a temporal point of view, this biphasic $[Ca^{2+}]_{IC}$ response is well in accordance with the biphasic insulin release observed in vitro in isolated islets (Refs). As already mentioned, an initial transient increase in $[Ca^{2+}]_{IC}$ is followed by a sustained plateau phase with superimposed higher frequency $[Ca^{2+}]_{IC}$ oscillations. The frequency and duration of $[Ca^{2+}]_{IC}$ oscillations during the plateau phase in the slice preparation closely resemble those measured electrophysiologically in acutely dissected pancreatic islets (add Atwater et al., 1980) and in islets in tissue slices (). During the transient phase, the initial activation of cells varies greatly in time and space, and the activation is detected in small clusters of beta cells dispersed over an islet with no predictable pattern [add Dolensek et al 2013]. During the plateau phase, cells display synchronized calcium oscillations spreading repeatedly in a wave-like manner across islets with an average velocity of about 100 µm/s [add Stozer et al and Dolensek et al 2013]. Simultaneous measurements of membrane potential oscillations and calcium oscillations demonstrated tight coupling of the two processes (Gilon and Henquin 1992, Beauvois, Merezak et al. 2006), with membrane potential preceding the calcium increase by about 150 ms (Dolenšek, Stožer et al. 2013). After lowering glucose back to substimulatory concentration, beta cells in acute tissue slices deactivate, and their intracellular calcium concentration returns back to the pre-stimulatory level, but with a shorter delay and less heterogeneously than during the onset of the response (Stožer, Dolenšek et al. 2013, Stožer, Gosak et al. 2013, Markovic, Stozer et al. 2015).

An important hallmark of proper function in beta cells is the high level of cell-to-cell interactions within islets (Refs). Within areas of plasma membrane delimited by tight junctions, beta cells express gap junctions consisting of the connexin 36 protein that allows for electrical coupling and exchange of small signaling molecules between adjacent cells (Moreno, Berthoud et al. 2005, Cigliola, Chellakudam et al. 2013, Skelin Klemen, Dolenšek et al. 2017). Gap junctions along with other intercellular paracrine signaling mechanisms are thought to ensure coordinated cellular activity and warrant a well-regulated secretion of insulin at elevated glucose levels (Bosco, Haefliger et al. 2011, Benninger and Piston 2014).

However, the functional beta cell networks extracted from calcium dynamics are much more heterogeneous as one would expect from a syncytium mediated by only gap junctions (Cherubini, Filippi et al. 2015, Barua and Goel 2016, Cappon and Pedersen 2016). More specifically, instead of being rather regular and lattice-like, the functional beta cell networks exhibit small-worldness and a clustered structure with well-pronounced subcompartments (Stožer, Gosak et al. 2013, Markovic, Stozer et al. 2015, Johnston, Mitchell et al. 2016, Gosak, Markovic et al. 2018, Nasteska and Hodson 2018). Moreover, the interplay between intrinsic cellular signaling characteristics, the network parameters, and responses to changes in stimulation with glucose is largely unexplored, especially at different glucose concentrations.

Although the role of intercellular communication in islet dysfunction is incompletely understood, more and more studies suggest that the coordinated activity within islets is not only important for normal insulin secretion dynamics but may be directly involved in the pathogenesis of diabetes mellitus (Hodson, Mitchell et al. 2013, Daraio, Bombek et al. 2017). Disruptions in gap junctional and paracrine communication abolish synchronized electrical and calcium activity and lead to altered plasma insulin oscillations and to glucose intolerance (Ravier, Güldenagel et al. 2005, Head, Orseth et al. 2012), as observed in numerous models of obesity and diabetes mellitus (Carvalho, Oliveira et al. 2012, Hodson, Mitchell et al. 2013, Benninger and Piston 2014). (Add Stamper et al Phys Rev E 2014)

The aim of this study was to systematically measure and analyze the dynamics of intracellular calcium oscillations in beta cells in acute pancreas tissue slices to assess different glucose-dependent properties, with a particular lookout for emergent collective operations in both physiological and supraphysiological glucose concentrations. For this, we recorded beta cell activation and deactivation as well as activity during plateau phase in a concentration-dependent manner, extracted and analyzed typical classical physiological and advanced network parameters, and finally compared the different properties of cells.

## 2. Materials and Methods

### 2.1.Ethics statement

The study was conducted in strict accordance with all national and European recommendations pertaining to care and work with experimental animals, and all efforts were made to minimize suffering of animals. The protocol was approved by the Veterinary administration of the Republic of Slovenia (permit number: U34401-12/2015/3).

### 2.2. Tissue slice preparation and dye loading

8-20 week old NMRI mice of either sex were kept on a 12:12 hours light: dark schedule in individually ventilated cages (Allentown LLC, USA) and used for preparation of acute pancreas tissue slices, as described previously (Speier and Rupnik 2003, Stožer, Dolenšek et al. 2013). In brief, after sacrificing the mice, we accessed the abdominal cavity via laparotomy and injected low-melting point 1.9 % agarose (Lonza, USA) dissolved in extracellular solution (ECS, consisting of (in mM) 125 NaCl, 26 $NaHCO_3$, 6 glucose, 6 lactic acid, 3 myo-inositol, 2.5 KCl, 2 Na-pyruvate, 2 $CaCl_2$, 1.25 $NaH_2PO_4$, 1 $MgCl_2$, 0.5 ascorbic acid) at 40 °C into the proximal common bile duct, which we clamped distally at the major duodenal papilla. Immediately after

injection, we cooled the agarose infused pancreas with ice-cold ECS and extracted it. We prepared tissue slices with a thickness of 140 µm with a vibratome (VT 1000 S, Leica) and collected them in HEPES-buffered saline at RT (HBS, consisting of (in mM) 150 NaCl, 10 HEPES, 6 glucose, 5 KCl, 2 $CaCl_2$, 1 $MgCl_2$; titrated to pH=7.4 using 1 M NaOH). For staining, we incubated the slices for 50 minutes at RT in the dye-loading solution (6 µM Oregon Green 488 BAPTA-1 AM (OGB-1, Invitrogen), 0.03% Pluronic F-127 (w/v), and 0.12% dimethylsulphoxide (v/v) dissolved in HBS). All chemicals were obtained from Sigma-Aldrich (St. Louis, Missouri, USA), unless otherwise specified.

### 2.3. Stimulation protocol and calcium imaging

Individual tissue slices were transferred to a perifusion system containing carbogenated ECS at 37 °C and exposed to single square pulse-like stimulation per slice (7, 8, 9, 12, or 16 mM, lasting 40, 30, 20, 15 and 15 minutes, respectively, followed by an incubation in a solution with substimulatory glucose concentration (6 mM) until all the activity switched off. The duration of a single stimulation pulse varied due to large differences in time needed to activate and deactivate beta cell networks at different glucose concentrations. We performed the imaging on a Leica TCS SP5 AOBS Tandem II upright confocal system (20x HCX APO L water immersion objective, NA 1.0) and a Leica TCS SP5 DMI6000 CS inverted confocal system (20X HC PL APO water/oil immersion objective, NA 0.7). Acquisition frequency was initially set to 1-2 Hz at 512 x 512 pixels during the first phase response, allowing for determination of response onsets and deactivation, and switched to 27 – 50 Hz at 128 x 128 pixels for intermittent sampling of the plateau phase to allow for precise quantification of $[Ca^{2+}]_{IC}$ oscillations. OGB-1 was excited by an argon 488 nm laser line and emitted fluorescence was detected by Leica HyD hybrid detector in the range of 500-700 nm (all from Leica Microsystems, Germany), as described previously (Stožer, Dolenšek et al. 2013).

### 2.4. Data analyses

We manually selected ROIs and exported traces for an off-line analysis utilizing a custom-made software application (name, copyright). We excluded recordings with extensive motion artefacts. Further off-line analysis of $[Ca^{2+}]_{IC}$ traces was made using in-house MATLAB/Python scripts. Fluorescence signals were expressed as $F/F_0$, the ratio of fluorescence signal (F) at an individual time point of the experiment relative to the initial level of fluorescence ($F_0$). To account for photobleaching, we used a combination of linear and exponential fitting. The methodology used to determine $[Ca^{2+}]_{IC}$ signal characteristics, e.g., the duration of oscillations, which was established at half maximal amplitude of the spike, the number of oscillations per minute, and the percentage of active time, is described in detail in the respective figures and figure captions. The activation times and deactivation times, i.e. the starts of calcium increases/decreases after switching from basal to stimulatory concentration (and vice versa), were selected manually. Two cells were considered to be in the same activation/deactivation cluster, if their activation/deactivation times were less than 3 seconds apart, based on the average estimated speed of $[Ca^{2+}]_{IC}$ oscillation spreading across the islets [add Dolensek et al 2013]. For examining possible correlations between different spatiotemporal signaling characteristics, we used normalized ranks for all parameters (frequency, node degree, etc.). Statistics were calculated using SigmaPlot. Statistical differences between groups were tested

using ANOVA on Ranks and posthoc Dunn's method, and difference between two groups using the Mann-Whitney U test. Pearson correlation coefficient was calculated for correlations, and its significance tested by the z-score. Asterisks denote statistically significant differences, as follows: * $p<0.05$, ** $p<0.01$, and *** $p<0.001$.

### 2.5. Network analyses

To quantify the collective activity of the beta cell population in each islet, we constructed functional connectivity networks . Two cells were considered to be functionally connected if their activity profiles exceeded a preset degree of synchronization, as described elsewhere (Hodson, Mitchell et al. 2013, Stožer, Gosak et al. 2013, Gosak, Markovic et al. 2018). The resulting functional networks were diagnosed with conventional network metrics. More specifically, to explore the connectivity of cells, we calculated the average degree and the relative degree distribution. For the evaluation of the network's traffic capacity and functional integration of individual cells, we computed the global efficiency and the largest component. To characterize the functional segregation, we calculated the clustering coefficient and modularity, which reflect the level of clique-like structures within interconnected cell assemblies and the extent of division into smaller subpopulations, respectively. For details see (Boccaletti, Latora et al. 2006) (Gosak, Markovic et al. 2018).

## 3. Results

Beta cell networks within an islet were tested for concentration-dependence using square pulse transient elevations to a range of concentrations above the threshold typically encountered in normal mice *in vivo* (7, 8 , and 9 mM), as well as to two concentrations (12 and 16 mM) that lie within the range usually encountered in diabetic mice and in most of the previous studies. A response of a typical beta cell in a network to a stimulus protocol consisted of three subsequent phases: (i) activation, (ii) plateau, and (iii) deactivation (Figs. 1 and 5).

### *3.1 Glucose-dependence of beta cell activation*

The spatiotemporal activation properties of individual beta cells in an optical plane were examined following stepwise glucose increases from 6 mM to 7, 8, 9, 12, or 16 mM. Each islet was stimulated with a single stimulatory condition. Beta cells responded to the given glucose concentration with a characteristic delay in the onset of $[Ca^{2+}]_{IC}$ increase (activation delay) that progressively shortened with increasing glucose concentrations (Fig. 1C). Strikingly, the median beta cell activation delay was more than 15 min (916 s) at the threshold concentration of 7 mM glucose and progressively decreased to only approximately 2 min (121 s) at 16 mM glucose (Figure 1C). We observed a large degree of heterogeneity in delays among individual cells and cell clusters at a given glucose concentration. Interestingly, this heterogeneity was also glucose-dependent, exemplified by progressively shorter lags between the response of the first-responding cell in a given islet and the response of any other cell (cell-cell delay; Figure 1A-B).More specifically, the interquartile range in first cell-any cell delays decreased from around 7 minutes (443 s) in 7 mM glucose to about half a minute (36 s) in 16 mM glucose

(Fig. 1D). Consistent with the above findings, time points at which 50 % of cells were activated decreased progressively with increasing glucose concentrations (Figure 1E).

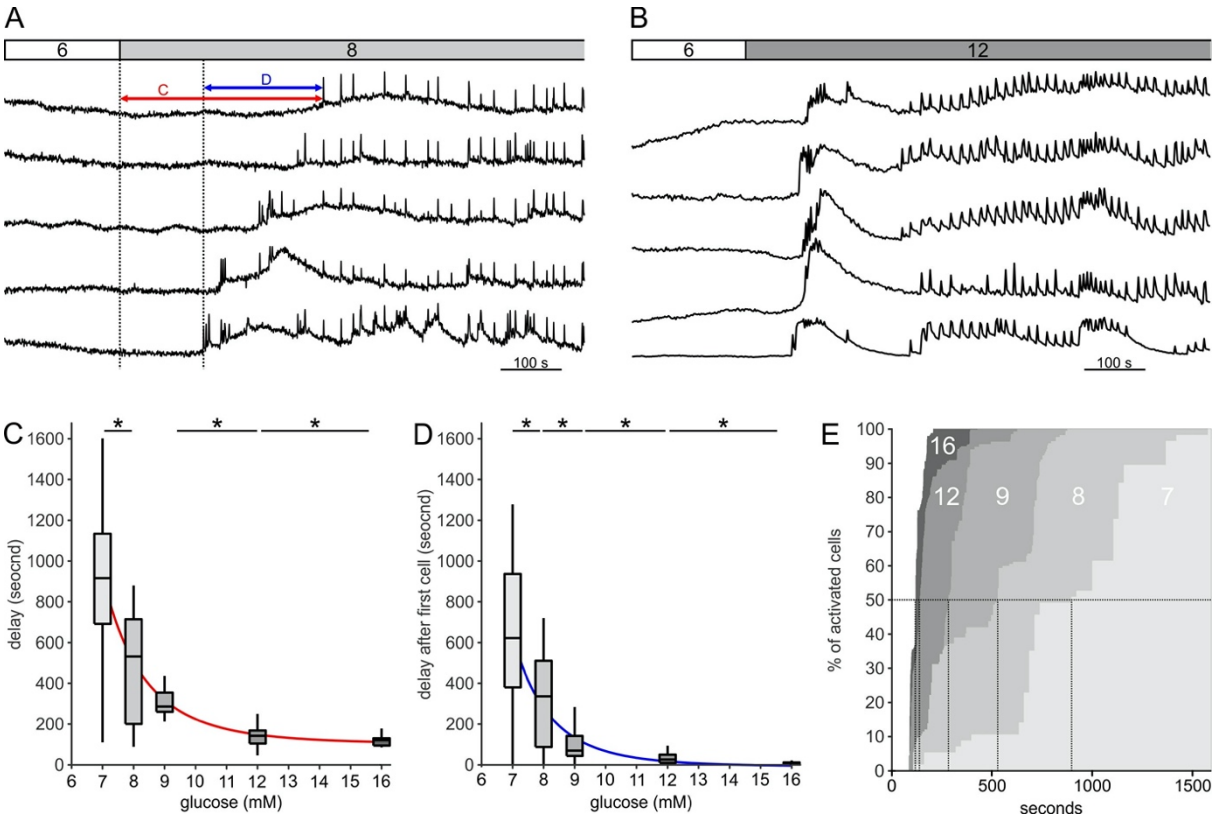


***Figure 1: Glucose-dependent activation.*** ***A*** *and* ***B*** *Response onsets of typical beta cells to stimulation with 8 mM (A) and 12 mM glucose (B). Lines indicate activation delays in individual cells (red line, pooled data shown in panel C) and variability of delays (blue line, pooled data shown in panel D).* ***C*** *Glucose-dependence of activation delays after stimulation with 7 mM, 8 mM, 9 mM, 12 mM, and 16 mM glucose.* ***D*** *Glucose-dependence of first cell-any cell delays.* ***E*** *Cumulative distributions of activation delays within islets. Vertical lines indicate the time at which half of the cells were activated at a given stimulus. Pooled data from 57 (16 mM), 167 (12 mM), 134 (9 mM), 371 (8 mM), and 231 (7 mM) cells, respectively, and from 2, 7, 2, 12, and 4 islets, respectively.*

As observed from Figure 1E, the activation of beta cells during stimulation had a staircase-like appearance, suggesting that groups of beta cells rather than single cells activated at the same time. Closer inspection of this pattern on the recorded time series revealed that beta cells formed spatiotemporal clusters of neighboring cells in response to glucose stimulation (Figure 2A-D). To quantify the relationship of cluster sizes to glucose concentration, we calculated the percentage of arbitrarily defined large clusters (>33 %, > 50%, and >67 %) for different glucose concentrations (Figure 2E). Increasing glucose concentration progressively increased the size of the clusters of activated cells, as demonstrated by the cumulative distribution of the cluster sizes for different concentrations of glucose (Figure 2F).

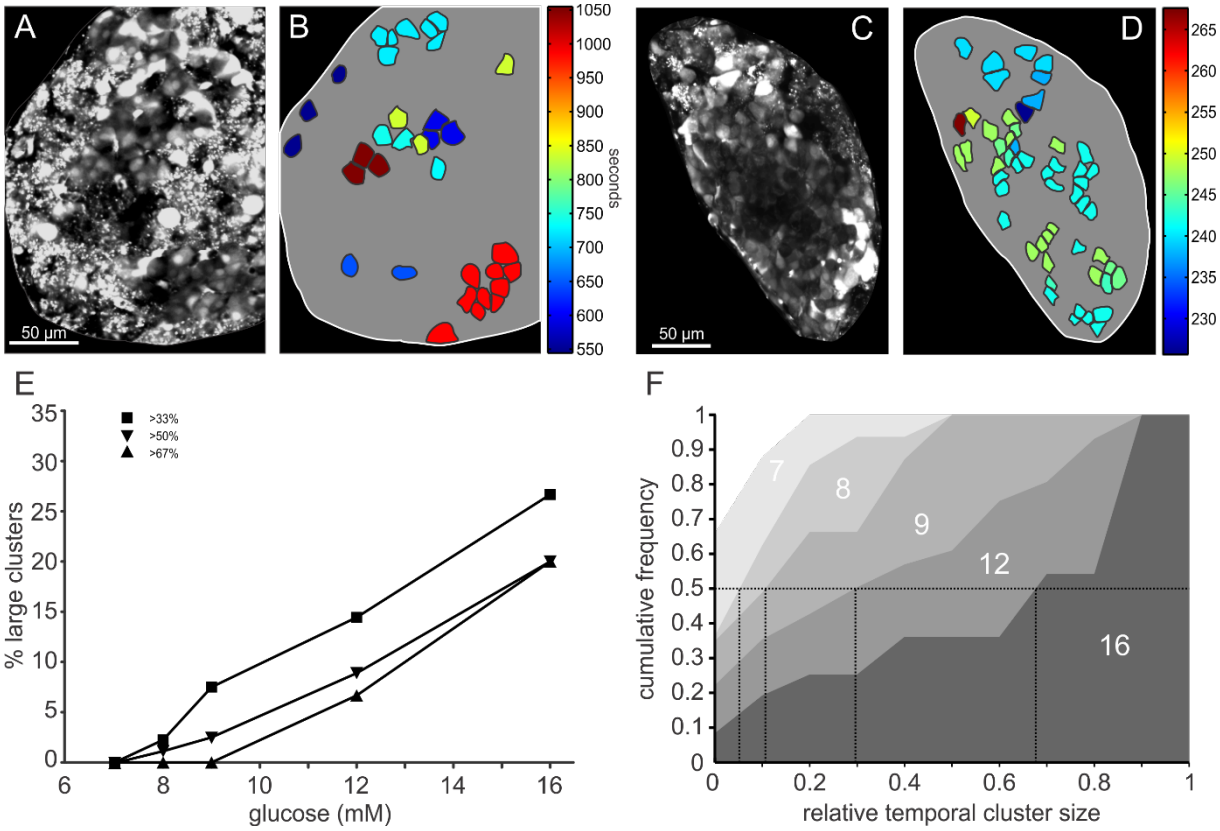


***Figure 2: Spatiotemporal characterization of beta cell activation: A-D*** *Color-coded response onset times of beta cells after 8 mM (B) and 12 mM (D) glucose stimulation. OGB-1 loaded cells in an islet are shown (A and C).* ***E*** *Distribution of relative sizes of clusters signifying simultaneously activated cells under stimulation with different concentrations of glucose.* ***F*** *Cumulative distribution of the relative cluster sizes for different glucose concentrations. Vertical lines indicate the relative temporal cluster size during activation of the first half of the cells in an islet.*

### *3.2 Glucose-dependent spatiotemporal $[Ca^{2+}]_{IC}$ dynamics during the plateau phase*

Following the initial transient calcium rise, the plateau phase was characterized by relatively regular high frequency $[Ca^{2+}]_{IC}$ oscillations that encompassed the majority of cells in an islet. This oscillatory activity was affected by progressively higher glucose concentrations (Figure 3). Comparing beta cell responses demonstrated that glucose modulated both frequency and duration of oscillations. More specifically, the frequency of oscillations increased steadily across the physiological range of glucose concentrations (7-9 mM, Figure 3A), reached its peak at 12 mM and decreased in 16 mM glucose (Figure 3 C). On the other hand, the duration of oscillations did not seem to be modulated at physiological glucose concentrations, but increased with the rise in glucose concentration to 12 and 16 mM glucose (Figure 3D). As a consequence, the relative active time, i.e., the percentage of time that cells spend in an increased $[Ca^{2+}]_{IC}$, was dominated by the increasing frequency of oscillations in the range from 7 to 9 mM glucose, and in higher concentrations by increasing durations of $[Ca^{2+}]_{IC}$ oscillations

(Figure 3E). An alternative presentation of active time concentration-dependence is presented graphically in Figure 3F, where average oscillation duration is plotted as a function of average interspike interval. Please note that the correlation slope reflecting the active time ($k = \frac{duration}{interspike\ interval} \sim duration \times frequency = active\ time$) increases with increasing glucose (Figure 3F).

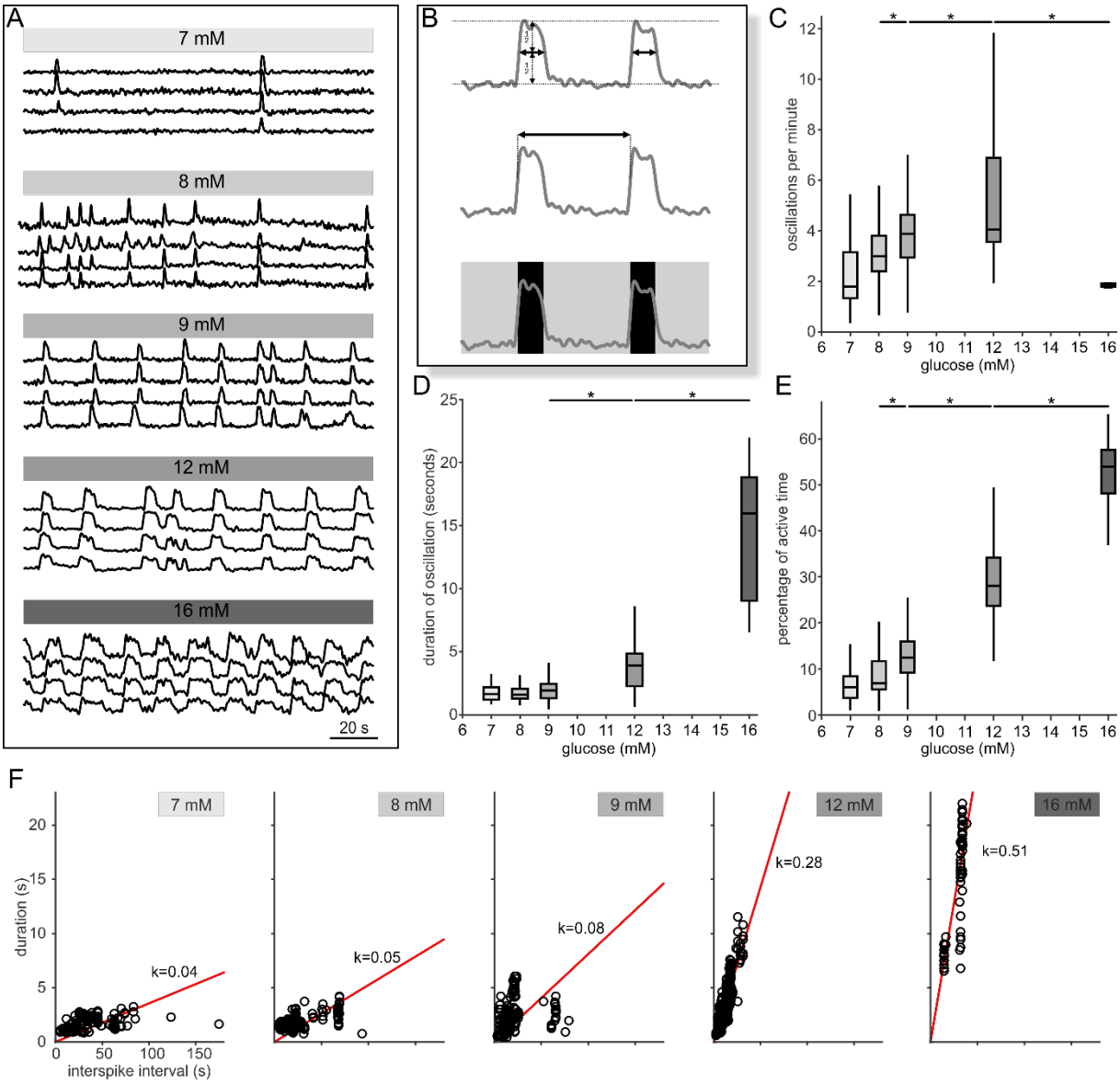


***Figure 3: Spatiotemporal characterization of the plateau phase. A*** *Oscillatory activity during stimulation with 7 mM, 8 mM, 9 mM, 12 mM, and 16 mM glucose. Shown are four cells from an islet per stimulus.* ***B*** *Schematic presentation of analyzed parameters: duration of oscillations at half-maximal amplitude (upper panel), number of oscillations per minute (middle panel) and proportion of active time (lower panel).* ***C-E*** *Frequency of oscillations (C), duration of oscillations (D), and percentage of active time (E) as a function of stimulus concentration.* ***F*** *Durations of individual oscillation as a function of the respective interspike interval. Glucose concentrations and slopes (k) of linear regression lines are indicated. $R^2$ = 0.72, 0.80, 0.59, 0.95,*

*and 0.96 for 7, 8, 9, 12, and 16 mM glucose, respectively (p<0.001). For all panels, data are pooled for 7 mM, 8 mM, 9 mM, 12 mM and 16 mM glucose from 4, 3, 9, 10 and 2 mice, from 5, 7, 14, 16 and 3 islets, and from 136, 241, 241, 392 and 62 cells, respectively.*

To further characterize beta cell collective behavior during the plateau phase, functional networks of beta cells were constructed for each glucose concentration, as described in Methods (Figure 4). As already previously shown , the functional connectivity of beta cells within an islet evolved with increasing stimulatory glucose concentrations. Stimulation with low glucose concentrations (7 or 8 mM) yielded mostly isolated and seldomly synchronized activity of beta cells. An increase in stimulatory glucose resulted in greater coordination of cellular activity within an islet, demonstrated by the increasing density of networks (Figure 4A-E), and greater average correlation in activity and node degree (Figure 4G and H). The increase in synchronization can be explained not only by an increase in activity, i.e., greater number of calcium oscillations, but also by an increased number of cells involved in individual oscillations. The relative degree distributions for different glucose concentrations presented in Figure 4F show that beta cell networks are in general very heterogeneous. Except for very high glucose concentrations, a relatively small fraction of cells exist, which are very well connected. These cells are functionally correlated with 20-30 % of the islet at exposure to 7 and 8 mM glucose concentration, and up to 60 % at 9 and 12 mM glucose. At 16 mM, the network becomes very dense as it has a high number of highly connected cells (Figure 4E and H). Intense stimulation diminishes the intrinsic cellular variability and the spatiotemporal activity is dominated by global and fully synchronized $[Ca^{2+}]_{IC}$ oscillations. Increasing glucose concentrations also resulted in functional networks that were more integrated locally, illustrated by an increase in average clustering (Figure 4J), as well as globally, demonstrated by decreased modularity (Figure 4K). Moreover, the increase in glucose concentration led to formation of more robust networks with higher functional integration, as can be seen from an increase in both the relative largest component and global efficiency in Figures 4I and 4L, respectively. Node degree of beta cells within networks were in general not at all correlated with any of the plateau activity properties (frequency, duration, or active time of oscillations, Figure S1). Similar lack of correlation was observed when comparing activation properties during initial glucose-dependent activation with the plateau phase response properties of the same beta cell (Figure S2).

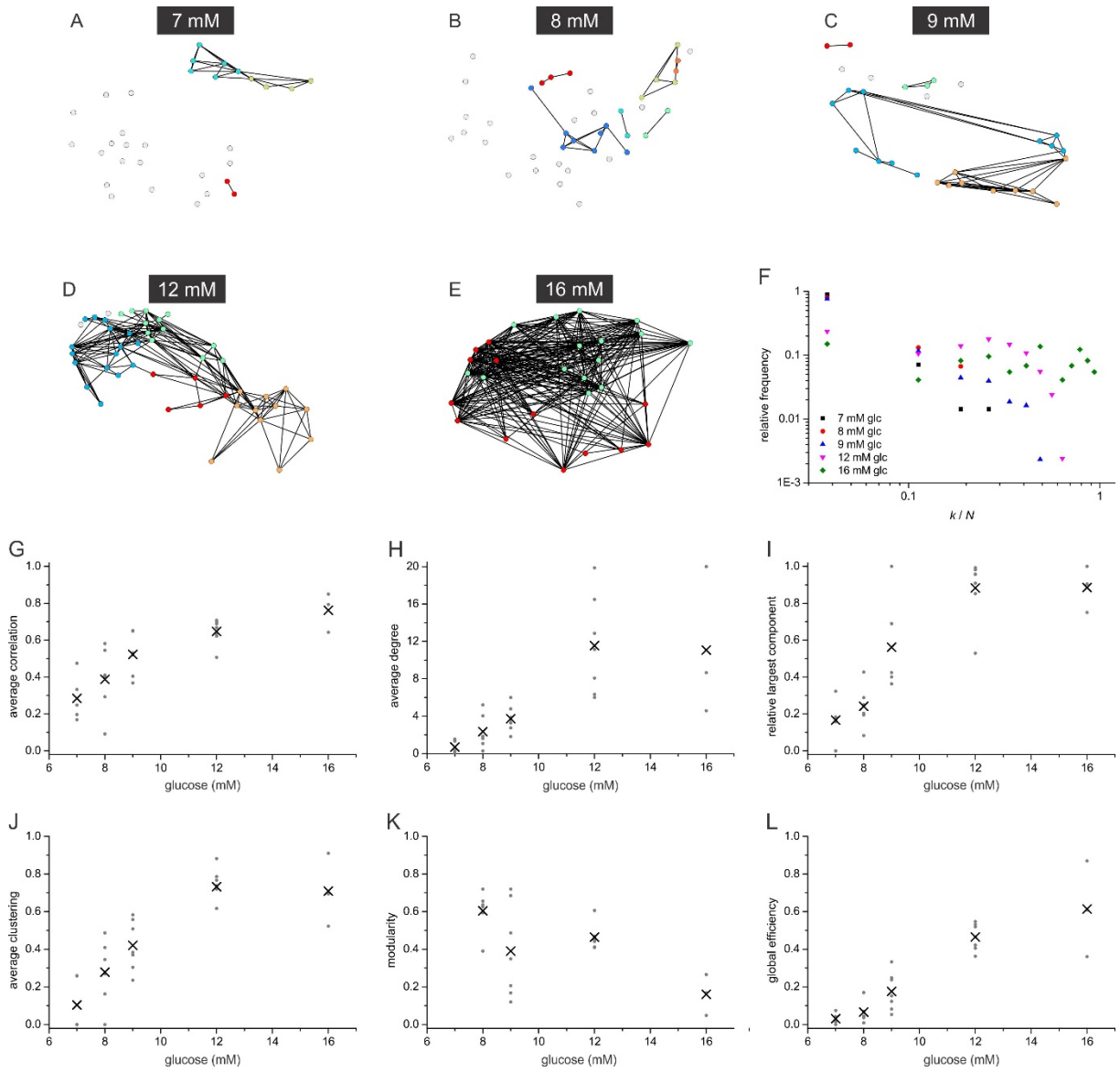


***Figure 4: Beta cell functional connectivity at different glucose concentrations. A-E*** *Characteristic functional networks for 7 mM (A), 8 mM (B), 9 mM (C), 12 mM (D), and 16 mM glucose (E).* ***F*** *Relative degree distributions at different glucose concentrations combined and normalized for all functional networks at given stimulatory conditions.* ***G-L*** *Synchronization and network metrics as a function of stimulatory glucose concentrations: average correlation coefficient (G), average network degree (H), relative largest component (I), average clustering coefficient (J), modularity (K), and global efficiency (L). Grey dots indicate values from individual islets and the black crosses the averages over all islets at a given concentration.*

### *3.3 Glucose-dependence of beta cell deactivation*

Removal of stimulatory glucose concentrations caused a concentration-dependent deactivation of beta cells (Figure 5). Concentration-dependence was observed primarily with respect to delays in onset of deactivation (deactivation delay), which were less than 3 min (median delay 174 s) at 7 mM glucose. Exposure to higher glucose concentrations caused beta cells to be active progressively longer after removal of stimulation, with the delay reaching a maximal value of about 15 min (median delay 896 s) at 16 mM (Figures 5C and E). A trend

towards glucose-dependence was also observed with respect to the variability of deactivation within islets (delay after first cell; Figure 5D). Finally, half-deactivation times were longer in in higher glucose concentrations (Figure 5 E).

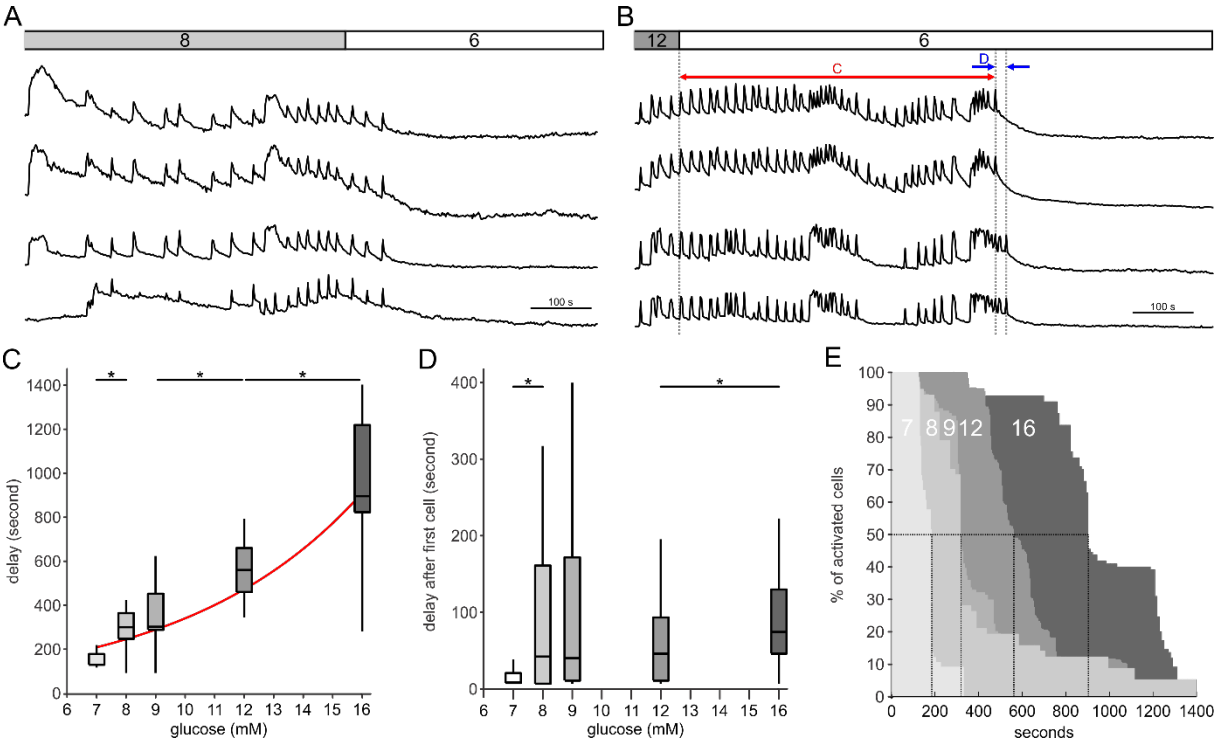


***Figure 5: Glucose-dependent deactivation . A-B*** *Deactivation of beta cells after cessation of stimulation with 8 mM (A) and 12 mM (B) glucose. Lines indicate deactivation delays in individual cells (red, pooled data shown in panel C) and any-cell-first-cell deactivation delays (blue, pooled data shown in panel D).* ***C*** *Deactivation delays in the deactivation of beta cells after cessation of stimulation with 7 mM, 8 mM, 9 mM, 12 mM, and 16 mM glucose. Data pooled from 66, 57, 134, 366 and 110 cells, from 3, 3, 2, 12, and 5 islets, and from 2, 2, 2, 9, and 3 mice, respectively.* ***D*** *Cell-cell deactivation delays between the first deactivated cell and any given cell from the same islet.* ***E*** *Cumulative distributions of delays between the end of stimulation and deactivation of any given cell. Vertical lines indicate the time at which half of the cells deactivated at a given stimulus.*

As with activation, deactivation occurred in glucose-dependent spatiotemporal clusters (Figure 6), a phenomenon observed at threshold stimulatory concentrations (Figure 6A and B), as well as supraphysiological stimulatory concentrations (Figure 6C and D). Exposure to lower stimulatory glucose concentrations evoked a small number of larger temporal clusters of deactivation. In contrast, a larger number of smaller temporal clusters were observed for high concentrations of stimulatory glucose (Figures 6E-F). Additionally, no correlation between deactivation and activation time ranks of cells was observed, neither at 8 mM nor at 12 mM glucose (Figure 7). Deactivation times of beta cells were only weakly correlated with some plateau phase properties (frequency, duration, active time, and node degree, Figure S3).

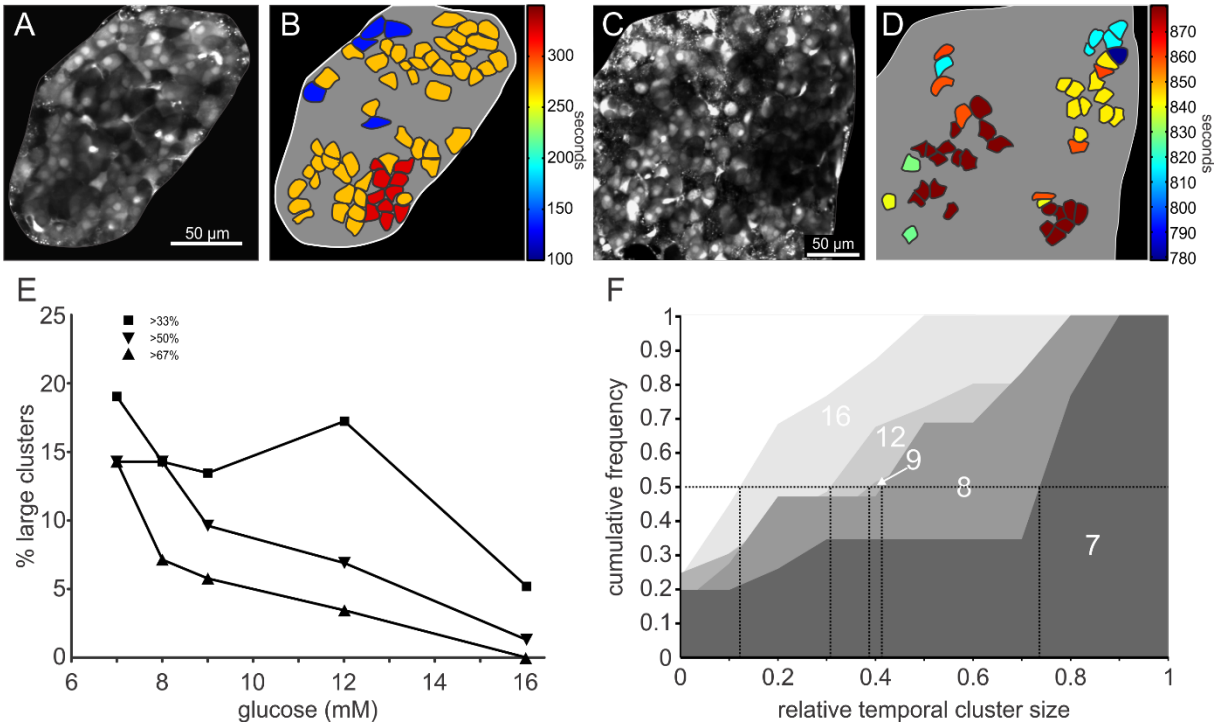


***Figure 6: Spatiotemporal characterization of beta cell deactivation. A-D*** *Color-coded response deactivation after cessation of 8 mM (B) and 12 mM (D) glucose stimulation. Loading of cells with OGB-1 is shown for respective islets (A and C).* ***E*** *Distribution of relative sizes of clusters signifying simultaneously deactivated cells after end of glucose stimulation.* ***F*** *Cumulative distribution of relative cluster sizes. Vertical lines indicate the relative temporal cluster size during deactivation of the first half of the beta cells in an islet.*

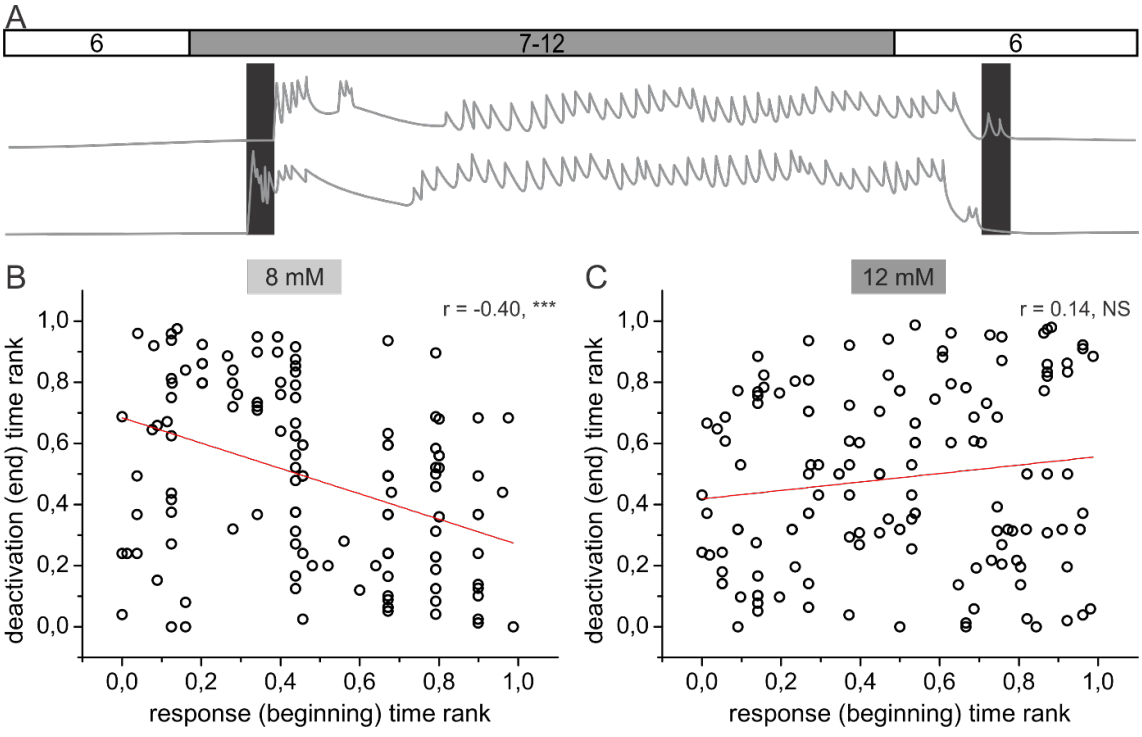

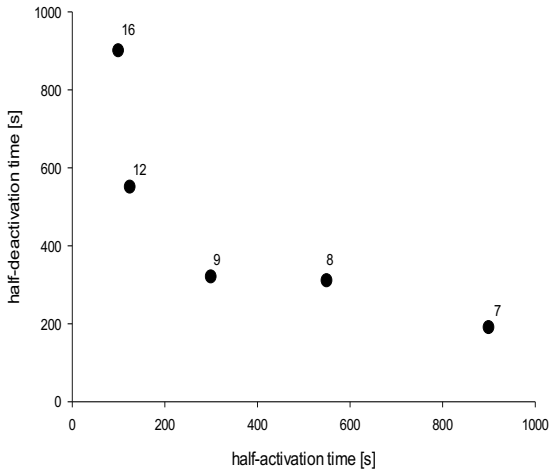


***Figure 7. The relationship between response half-activation and half-deactivation time..***

## 4. Discussion

In this paper, we aimed to assess the glucose-dependence of different beta cell classical and network functional parameters. To this goal, we systematically measured activation, plateau activity and functional beta cell network properties during this activity, as well as deactivation of beta cells in intact islets in acute tissue slices. We will now first discuss the little known patterns of heterogeneity apparent during the transient activation period of beta cells after stimulation with different glucose concentrations. We will then continue discussing the role of cell-cell interactions determining the rate of the activation in an islet as well as the size of the activating beta cell clusters during this process. A similar although inverse mechanism is in action during beta cell deactivation after the end of glucose stimulation. The coding for this inverse relation between activation and deactivation is happening on the level of beta cell collectives, rather than in single beta cells. Next, we will discuss dual coding of glucose stimulus contributing to the almost linear relationship between glucose concentration and active time, which stretches over a wide range of glucose concentrations. Finally, we will discuss the glucose dependence of beta cells collectives as complex networks and the general dissociation between the plateau activity parameters and beta cells activation as well as deactivation processes.

Little attention has so far been given to the transient activation period of individual beta cells within an islet. The heterogeneity of beta cells during the activation process was largely neglected as activation appears either sufficiently synchronous among cells (Bertuzzi, Davalli et al. 1999) or varied to some degree (Gilon and Henquin 1992, Jonkers and Henquin 2001, MacDonald and Rorsman 2006, Hodson, Mitchell et al. 2013, Do, Low et al. 2014). In either case, no systematic analysis of this parameter has been performed so far. One of the major reasons for the general lack of interest is that the glucose concentration used in most experiments to stimulate beta cells has been and still is today, a high supraphysiological

concentration (> 15 mM glucose), where also in our hands, activation happens in a most synchronous fashion (Figure 1 E). Such synchronous activation fits well with the general belief that closure of ATP-dependent $K^+$ channels causes simultaneous depolarization of beta cells, coupled into a functional syncytium (add Masa Islets). On the other hand, however, at physiological glucose concentrations (~8 mM glucose), the transient activation phase is prolonged, lasting longer than 10 minutes . This indicates a large degree of functional heterogeneity among beta cells or cell clusters. The idea of heterogeneity among beta cells has been around for decades (add Pipeleers). However, only recent experiments started to yield a large volume of evidence on its different flavors, be it in morphology (Bonner-Weir, Sullivan et al. 2015, Dolensek, Rupnik et al. 2015), protein and gene expression (Baron, Veres et al. 2016, Muraro, Dharmadhikari et al. 2016), connectivity (Rutter and Hodson 2013, Benninger and Piston 2014), or functional heterogeneity of both mouse and human beta cells (add some of Pats work). The activation process at the physiological glucose levels is actually so slow and limited to such small clusters of beta cells that it is plausible to question the prevailing view on the triggering pathway as a dominant on or off process in beta cell activation under physiological circumstances. Undoubtedly, physiological or pharmacological closure of KATP channels is one of the key events to activate beta cells. However, the present results strongly underline the important roles of intercellular coupling and recruitment as crucial events early during stimulation with physiological concentrations of glucose. Importantly, we showed previously that during periodic glucose stimulation protocols, which should more closely reflect physiological stimulation of beta cell collectives, beta cells do not synchronize to the level where $[Ca^{2+}]_{IC}$ oscillations would spread over the entire islet (Refs SOC1, SOC2).

We therefore want to emphasize that beta cells within an islet, although functionally coupled, shall not be regarded as a single functional unit in which each single cell displays almost identical and completely synchronous activation, plateau phase activity (Markovic, Stozer et al. 2015), and deactivation. After reaching the glucose concentration just above the physiological threshold, it takes some tens of minutes and a constantly elevated glucose level until all of numerous small clusters of beta cells distributed all over the islet eventually get activated into an active collective with a “wave-like” pattern, with spreading of the $[Ca^{2+}]_{IC}$ signal among the beta cells in the form of clear $[Ca^{2+}]_{IC}$ waves (Palti, BenDavid et al. 1996, Benninger, Zhang et al. 2008, Dolenšek, Stožer et al. 2013, Stožer, Dolenšek et al. 2013). In our hands, at this low stimulatory glucose concentration, an average beta cell spent less than 10 % of time in an active state within a rather segregated network with a limited number of strong interactions (Figure 4). When stimulatory levels of glucose were removed, such a collective of beta cells deactivated rapidly (Figures 5 and 7). On the other hand, collectives stimulated with supraphysiologically high glucose concentrations rapidly achieved the collective activation, spent more than 50 % of their time in an active state, but deactivated more slowly and gradually (Figs. 2, 5 and 7). Despite the evident negative correlation between activation and deactivation times at various glucose concentrations observed for the whole islet (Figure 7 D), detailed analysis on the level of individual cells or strongly interacting cell-pairs in a beta cell network showed that there was no such correlation between activation and deactivation ranks. In other words, a beta cell that activated among the first did not

necessarily deactivate among the first or the last during deactivation. Similarly, there was no correlation between classic and network parameters of activity during the plateau and activation as well as deactivation phase. Our data suggest that activation and deactivation properties are a collective trait that could not be picked up on the level of individual cells or analysis of predominantly strong cell-cell interactions between network nodes only. Single cell resolution functional measurement of metabolic profiles or molecular snapshots following an experiment like performed for this study shall yield the information on how or if at all, either metabolic state or protein expression patterns fit the pattern of beta cell activation and deactivation. Furthermore, it is important to mention that beta cells are not a homogenous population within the whole animal. Rather, they form complex and multilayered system composed of subpopulations of islets within a pancreas (Ellenbroek, Töns et al. 2013, Zhu, Larkin et al. 2016), and on the next lower level of complexity also subpopulations of beta cells within an islet (Benninger and Hodson 2018, Nasteska and Hodson 2018). To complicate matters further, maturation of beta cells within an islet can change their metabolic status and physiological features (Bader, Migliorini et al. 2016). Current technology enables us to use computational analyses, like random matrix theory, on available datasets to readily segment functional heterogeneity of a single islet (add Korosak and Rupnik ArXiv or Frontiers 2019).

Beta cell neighborhood within an islet appears to have a role in determining its activation profile (Figure 2). Activation is confined to small clusters of nearby cells with no predictable spatial pattern. The size of clusters increased with the glucose concentration indicating that the coupling between cells was affected by the glucose stimulus. Indeed, several studies suggested that glucose (Benninger, Hutchens et al. 2014) and sulphonylureas (Meda, Orci et al. 1984) affect the extent of coupling between beta cells directly. Alternatively, in electrically coupled cellular systems, the increased input resistance due to closure of $K^+$ or in fact any ion channel in plasma membrane, increases the length constant for the transfer of a signal between the coupled cells, without a direct change in coupling extent. As the synchronization of beta cells within an islet depends on the extent of coupling (Calabrese, Zhang et al. 2003, Benninger, Zhang et al. 2008, Benninger and Piston 2014) these two alternatives could provide a plausible mechanism for the concentration-dependence of the activation delays.

A hallmark of the plateau phase occurring during sustained stimulation with glucose, are repetitive fast $[Ca^{2+}]_{IC}$ oscillations. Few studies attempted to decipher how glucose modulates dynamics of calcium oscillations, yielding contradictory results, likely due to different glucose ranges tested. Microelectrode array study demonstrated that within the physiological concentration range glucose increased frequency only (Lebreton, Pirog et al. 2015), and sharp electrode and calcium imaging studies demonstrated that supraphysiological concentrations affected oscillation duration with little effect on the frequency (Meissner and Schmelz 1974, Henquin 1992, Barbosa, Silva et al. 1998, Antunes, Salgado et al. 2000). In the present paper, we demonstrate that the pattern of $[Ca^{2+}]_{IC}$ oscillations tightly depends on the stimulus intensity, and, most importantly, the relation to the stimulus intensity shows dual coding properties (Figure 3). More specifically, within physiological limits of glucose concentrations, the frequency of oscillations follows the increase in the glucose concentration. At higher

glucose concentrations, the active time of beta cells is dominated by an increase in the duration of oscillations rather than their frequency. Previously, the dual coding properties of beta cells could only be inferred implicitly, for the lack of systematic analysis of frequencies and durations, or for the fact that too few concentrations were tested to scrutinize the coding properties. Combinatorial effect of increasing frequency and duration resulted in our study in an almost linear increase in active time over a wide range of glucose concentrations (Figure 3), a feature also picked up in studies utilizing microdissected islets (Cook and Ikeuchi 1989, Henquin 1992). Active time thus serves as an excellent predictor of the amount of insulin secreted, as (i) electrical activity and calcium influx are closely related to insulin secretion (Ammälä, Eliasson et al. 1993, Barbosa, Silva et al. 1998, Satin 2000), and (ii) there is tight synchronization between calcium and insulin oscillations within a single beta cell (Gilon, Shepherd et al. 1993). The aforementioned proportional increase in insulin release stretching high into the range of nonphysiologically high glucose concentrations (Ashcroft, Bassett et al. 1972, Gao, Drews et al. 1990, Detimary, Jonas et al. 1995, Henquin, Nenquin et al. 2006, Benninger, Head et al. 2011, Low, Mitchell et al. 2013) has been integrated into the so called metronome hypothesis, which predicts that an increase in glucose increases the plateau fraction of the calcium oscillations, ultimately leading to an increase in the amplitude of insulin pulses (Satin, Butler et al. 2015). The described mechanisms most probably also involve increased mobilization and priming of insulin granules (Pedersen, Tagliavini et al. 2019).

There is accumulating evidence that beta cells within an islet participate in a rich signal exchange with their neighbors, forming an electrically and chemically coupled network. Gap junctional coupling via connexin 36 proteins stands for short-range interactions, whereas the paracrine and cholinergic signaling mechanisms ensure also long-range interactions between cells (Zhang, Galvanovskis et al. 2008, Rutter and Hodson 2013, Molina, Rodriguez-Diaz et al. 2014). For a long time we though that these mechanisms ensure the necessary means to overcome the heterogeneity of beta cells and enable high level of synchronous activity. In contrary, at physiological glucose levels beta cells are not completely synchronized and the resulting spatiotemporal dynamics is complex. The question arises to what extent the highly synchronous activity is necessary for normal physiology of beta cells and to what extent is the driving of beta cells into such synchronous activity using pharmacological tools reasonable for their long-term function and survival (add ref from Nature medicine Ecki)?

Advanced network analyses based on thresholded pairwise correlations of $Ca^{2+}$ imaging signals have proven to be a valuable tool to quantify the non-trivial intercellular interaction patterns in multicellular systems (Stetter, Battaglia et al. 2012, Feldt Muldoon, Soltesz et al. 2013), including the pancreatic islets (Hodson, Mitchell et al. 2013, Stožer, Gosak et al. 2013, Markovic, Stozer et al. 2015, Johnston, Mitchell et al. 2016, Gosak, Markovic et al. 2018). These endeavors have been at least in part motivated by the fact that the arrangement and communication abilities between beta cells is an increasingly popular topic in islet and diabetes research, not only because its critical role in insulin release through the generation of coordinated rhythmic activity (Bavamian, Klee et al. 2007, Cigliola, Chellakudam et al. 2013, Benninger and Piston 2014, Rutter and Hodson 2014), but also due to the growing evidence that connectivity may plausibly be targeted by both environmental and genetic factors in the pathogenesis of diabetes mellitus (Hodson, Mitchell et al. 2013, Farnsworth, Walter et al.

2016, Westacott, Farnsworth et al. 2017). In the present study we pushed further our understanding of beta cell networks by exploring the glucose dependencies of intercellular behavior and by connecting the network properties with cellular signaling characteristics. Our results revealed that for physiological concentrations of glucose the functional networks are quite segmented, locally clustered and heterogeneous, whereas supraphysiological stimulation levels lead to globally more synchronized behavior and hence to denser and more integral and efficient networks, which corroborates previous undertakings (Gosak, Markovic et al. 2018). Moreover, mechanism governing the dynamics during the plateau phase seemed separate from the ones during activation and deactivation, as we could not detect any correlation between the plateau phase properties (frequency, duration, and network metrics) and activation (Figure S2) or deactivation (Figure S3).

References

Ammälä, C., L. Eliasson, K. Bokvist, O. Larsson, F. M. Ashcroft and P. Rorsman (1993). "Exocytosis elicited by action potentials and voltage-clamp calcium currents in individual mouse pancreatic B-cells." J Physiol **472**(1): 665-688.

Antunes, C. M., A. P. Salgado, L. M. Rosário and R. M. Santos (2000). "Differential patterns of glucose-induced electrical activity and intracellular calcium responses in single mouse and rat pancreatic islets." Diabetes **49**(12): 2028-2038.

Ashcroft, F. M. and P. Rorsman (1989). "Electrophysiology of the pancreatic beta-cell." Prog Biophys Mol Biol **54**(2): 87-143.

Ashcroft, S. J., J. M. Bassett and P. J. Randle (1972). "Insulin secretion mechanisms and glucose metabolism in isolated islets." Diabetes **21**(2 Suppl): 538-545.

Bader, E., A. Migliorini, M. Gegg, N. Moruzzi, J. Gerdes, S. S. Roscioni, M. Bakhti, E. Brandl, M. Irmler, J. Beckers, M. Aichler, A. Feuchtinger, C. Leitzinger, H. Zischka, R. Wang-Sattler, M. Jastroch, M. Tschop, F. Machicao, H. Staiger, H. U. Haring, H. Chmelova, J. A. Chouinard, N. Oskolkov, O. Korsgren, S. Speier and H. Lickert (2016). "Identification of proliferative and mature beta-cells in the islets of Langerhans." Nature **535**(7612): 430-434.

Barbosa, R. M., A. M. Silva, A. R. Tomé, J. A. Stamford, R. M. Santos and L. M. Rosário (1998). "Control of pulsatile 5-HT/insulin secretion from single mouse pancreatic islets by intracellular calcium dynamics." J Physiol **510**(1): 135-143.

Baron, M., A. Veres, S. L. Wolock, A. L. Faust, R. Gaujoux, A. Vetere, J. H. Ryu, B. K. Wagner, S. S. Shen-Orr, A. M. Klein, D. A. Melton and I. Yanai (2016). "A Single-Cell Transcriptomic Map of the Human and Mouse Pancreas Reveals Inter- and Intra-cell Population Structure." Cell Syst **3**(4): 346-360.e344.

Barua, A. K. and P. Goel (2016). "Isles within islets: The lattice origin of small-world networks in pancreatic tissues." Physica D: Nonlinear Phenomena **315**: 49-57.

Bavamian, S., P. Klee, A. Britan, C. Populaire, D. Caille, J. Cancela, A. Charollais and P. Meda (2007). "Islet-cell-to-cell communication as basis for normal insulin secretion." Diabetes, Obesity and Metabolism **9**: 118-132.

Beauvois, M. C., C. Merezak, J.-C. Jonas, M. A. Ravier, J.-C. Henquin and P. Gilon (2006). "Glucose-induced mixed [Ca2+]c oscillations in mouse β-cells are controlled by the membrane potential and the SERCA3 Ca2+-ATPase of the endoplasmic reticulum." American Journal of Physiology - Cell Physiology **290**(6): C1503-C1511.

Benninger, R. K., T. Hutchens, W. S. Head, M. J. McCaughey, M. Zhang, S. J. Le Marchand, L. S. Satin and D. W. Piston (2014). "Intrinsic islet heterogeneity and gap junction coupling determine spatiotemporal ca(2+) wave dynamics." Biophys J **107**(11): 2723-2733.

Benninger, R. K. and D. W. Piston (2014). "Cellular communication and heterogeneity in pancreatic islet insulin secretion dynamics." Trends Endocrinol Metab.

Benninger, R. K., M. Zhang, W. S. Head, L. S. Satin and D. W. Piston (2008). "Gap junction coupling and calcium waves in the pancreatic islet." Biophys J **95**(11): 5048-5061.

Benninger, R. K. P., W. S. Head, M. Zhang, L. S. Satin and D. W. Piston (2011). "Gap junctions and other mechanisms of cell–cell communication regulate basal insulin secretion in the pancreatic islet." J Physiol **589**(22): 5453-5466.

Benninger, R. K. P. and D. J. Hodson (2018). "New Understanding of β-Cell Heterogeneity and In Situ Islet Function." Diabetes **67**(4): 537-547.

Bergsten, P., E. Grapengiesser, E. Gylfe, A. Tengholm and B. Hellman (1994). "Synchronous oscillations of cytoplasmic Ca2+ and insulin release in glucose-stimulated pancreatic islets." Journal of Biological Chemistry **269**(12): 8749-8753.

Bertuzzi, F., A. M. Davalli, R. Nano, C. Socci, F. Codazzi, R. Fesce, V. Di Carlo, G. Pozza and F. Grohovaz (1999). "Mechanisms of coordination of $Ca^{2+}$ signals in pancreatic islet cells." Diabetes **48**(10): 1971-1978.

Boccaletti, S., V. Latora, Y. Moreno, M. Chavez and D. U. Hwang (2006). "Complex networks: Structure and dynamics." Physics Reports **424**(4–5): 175-308.

Bonner-Weir, S., B. A. Sullivan and G. C. Weir (2015). "Human Islet Morphology Revisited:Human and Rodent Islets Are Not So Different After All." Journal of Histochemistry & Cytochemistry **63**(8): 604-612.

Bosco, D., J.-A. Haefliger and P. Meda (2011). "Connexins: Key Mediators of Endocrine Function." Physiological Reviews **91**(4): 1393-1445.

Calabrese, A., M. Zhang, V. Serre-Beinier, D. Caton, C. Mas, L. S. Satin and P. Meda (2003). "Connexin 36 Controls Synchronization of Ca2+ Oscillations and Insulin Secretion in MIN6 Cells." Diabetes **52**(2): 417-424.

Cappon, G. and M. G. Pedersen (2016). "Heterogeneity and nearest-neighbor coupling can explain small-worldness and wave properties in pancreatic islets." Chaos **26**(5): 053103.

Carvalho, C. P. F., R. B. Oliveira, A. Britan, J. C. Santos-Silva, A. C. Boschero, P. Meda and C. B. Collares-Buzato (2012). "Impaired β-cell-β-cell coupling mediated by Cx36 gap junctions in prediabetic mice." American Journal of Physiology - Endocrinology And Metabolism **303**(1): E144-E151.

Cherubini, C., S. Filippi, A. Gizzi and A. Loppini (2015). "Role of topology in complex functional networks of beta cells." Phys Rev E Stat Nonlin Soft Matter Phys **92**(4-1): 042702.

Cigliola, V., V. Chellakudam, W. Arabieter and P. Meda (2013). "Connexins and β-cell functions." Diabetes Research and Clinical Practice **99**(3): 250-259.

Cook, D. L. and M. Ikeuchi (1989). "Tolbutamide as mimic of glucose on beta-cell electrical activity. ATP-sensitive K+ channels as common pathway for both stimuli." Diabetes **38**(4): 416-421.

Daraio, T., L. K. Bombek, M. Gosak, I. Valladolid-Acebes, M. S. Klemen, E. Refai, P. O. Berggren, K. Brismar, M. S. Rupnik and C. Bark (2017). "SNAP-25b-deficiency increases insulin secretion and changes spatiotemporal profile of Ca(2+)oscillations in beta cell networks." Sci Rep **7**(1): 7744.

Dean, P. M. and E. K. Matthews (1970). "Glucose-induced electrical activity in pancreatic islet cells." J Physiol **210**(2): 255-264.

Detimary, P., J. C. Jonas and J. C. Henquin (1995). "Possible links between glucose-induced changes in the energy state of pancreatic B cells and insulin release. Unmasking by decreasing a stable pool of adenine nucleotides in mouse islets." The Journal of Clinical Investigation **96**(4): 1738-1745.

Do, O. H., J. T. Low, H. Y. Gaisano and P. Thorn (2014). "The secretory deficit in islets from db/db mice is mainly due to a loss of responding beta cells." Diabetologia **57**(7): 1400-1409.

Dolensek, J., M. S. Rupnik and A. Stozer (2015). "Structural similarities and differences between the human and the mouse pancreas." Islets **7**(1): e1024405.

Dolenšek, J., A. Stožer, M. Skelin Klemen, E. W. Miller and M. Slak Rupnik (2013). "The Relationship between Membrane Potential and Calcium Dynamics in Glucose-Stimulated Beta Cell Syncytium in Acute Mouse Pancreas Tissue Slices." PLoS ONE **8**(12): e82374.

Ellenbroek, J. H., H. A. Töns, N. de Graaf, C. J. Loomans, M. A. Engelse, H. Vrolijk, P. J. Voshol, T. J. Rabelink, F. Carlotti and E. J. de Koning (2013). "Topologically Heterogeneous Beta Cell Adaptation in Response to High-Fat Diet in Mice." PLOS ONE **8**(2): e56922.

Farnsworth, N. L., R. L. Walter, A. Hemmati, M. J. Westacott and R. K. Benninger (2016). "Low Level Pro-inflammatory Cytokines Decrease Connexin36 Gap Junction Coupling in Mouse and Human Islets through Nitric Oxide-mediated Protein Kinase Cdelta." J Biol Chem **291**(7): 3184-3196.

Feldt Muldoon, S., I. Soltesz and R. Cossart (2013). "Spatially clustered neuronal assemblies comprise the microstructure of synchrony in chronically epileptic networks." Proc Natl Acad Sci U S A **110**(9): 3567-3572.

Fernandez, J. and M. Valdeolmillos (2000). "Synchronous glucose-dependent [Ca2+]i oscillations in mouse pancreatic islets of Langerhans recorded in vivo." FEBS Letters **477**(1–2): 33-36.

Gao, Z. Y., G. Drews, M. Nenquin, T. D. Plant and J. C. Henquin (1990). "Mechanisms of the stimulation of insulin release by arginine-vasopressin in normal mouse islets." J Biol Chem **265**(26): 15724-15730.

Gilon, P. and J. C. Henquin (1992). "Influence of membrane potential changes on cytoplasmic Ca2+ concentration in an electrically excitable cell, the insulin-secreting pancreatic B-cell." Journal of Biological Chemistry **267**(29): 20713-20720.

Gilon, P., R. M. Shepherd and J. C. Henquin (1993). "Oscillations of secretion driven by oscillations of cytoplasmic $Ca^{2+}$ as evidenced in single pancreatic islets." Journal of Biological Chemistry **268**(30): 22265-22268.

Gosak, M., R. Markovic, J. Dolensek, M. Slak Rupnik, M. Marhl, A. Stozer and M. Perc (2018). "Network science of biological systems at different scales: A review." Phys Life Rev **24**: 118-135.

Gylfe, E. (1988). "Nutrient secretagogues induce bimodal early changes in cytoplasmic calcium of insulin-releasing ob/ob mouse beta-cells." Journal of Biological Chemistry **263**(27): 13750-13754.

Head, W. S., M. L. Orseth, C. S. Nunemaker, L. S. Satin, D. W. Piston and R. K. Benninger (2012). "Connexin-36 gap junctions regulate in vivo first- and second-phase insulin secretion dynamics and glucose tolerance in the conscious mouse." Diabetes **61**(7): 1700-1707.

Henquin, J.-C. (2011). "The dual control of insulin secretion by glucose involves triggering and amplifying pathways in β-cells." Diabetes Research and Clinical Practice **93, Supplement 1**(0): S27-S31.

Henquin, J.-C., M. Nenquin, P. Stiernet and B. Ahren (2006). "In Vivo and In Vitro Glucose-Induced Biphasic Insulin Secretion in the Mouse." Diabetes **55**(2): 441-451.

Henquin, J. C. (1992). "Adenosine triphosphate-sensitive K+ channels may not be the sole regulators of glucose-induced electrical activity in pancreatic B-cells." Endocrinology **131**(1): 127-131.

Hodson, D. J., R. K. Mitchell, E. A. Bellomo, G. Sun, L. Vinet, P. Meda, D. Li, W. H. Li, M. Bugliani, P. Marchetti, D. Bosco, L. Piemonti, P. Johnson, S. J. Hughes and G. A. Rutter (2013). "Lipotoxicity disrupts incretin-regulated human beta cell connectivity." J Clin Invest **123**(10): 4182-4194.

Johnston, N. R., R. K. Mitchell, E. Haythorne, M. P. Pessoa, F. Semplici, J. Ferrer, L. Piemonti, P. Marchetti, M. Bugliani, D. Bosco, E. Berishvili, P. Duncanson, M. Watkinson, J. Broichhagen, D. Trauner, G. A. Rutter and D. J. Hodson (2016). "Beta Cell Hubs Dictate Pancreatic Islet Responses to Glucose." Cell Metab **24**(3): 389-401.

Jonkers, F. C. and J.-C. Henquin (2001). "Measurements of Cytoplasmic Ca2+ in Islet Cell Clusters Show That Glucose Rapidly Recruits β-Cells and Gradually Increases the Individual Cell Response." Diabetes **50**(3): 540-550.

Lebreton, F., A. Pirog, I. Belouah, D. Bosco, T. Berney, P. Meda, Y. Bornat, B. Catargi, S. Renaud, M. Raoux and J. Lang (2015). "Slow potentials encode intercellular coupling and insulin demand in pancreatic beta cells." Diabetologia.

Low, J. T., J. M. Mitchell, O. H. Do, J. Bax, A. Rawlings, M. Zavortink, G. Morgan, R. G. Parton, H. Y. Gaisano and P. Thorn (2013). "Glucose principally regulates insulin secretion in mouse islets by controlling the numbers of granule fusion events per cell." Diabetologia **56**(12): 2629-2637.

MacDonald, P. E. and P. Rorsman (2006). "Oscillations, Intercellular Coupling, and Insulin Secretion in Pancreatic β Cells." PLoS Biol **4**(2): e49.

Markovic, R., A. Stozer, M. Gosak, J. Dolensek, M. Marhl and M. S. Rupnik (2015). "Progressive glucose stimulation of islet beta cells reveals a transition from segregated to integrated modular functional connectivity patterns." Sci Rep **5**: 7845.

Meda, P., L. Orci, I. Atwater, A. Bangham, E. Rojas and A. Gonçalves (1984). "The Topography of Electrical Synchrony Among β-Cells in the Mouse Islet of Langerhans." Experimental Physiology **69**(4): 716-735.

Meissner, H. P. and H. Schmelz (1974). "Membrane potential of beta-cells in pancreatic islets." Pflügers Archiv European Journal of Physiology **351**(3): 195-206.

Molina, J., R. Rodriguez-Diaz, A. Fachado, M. C. Jacques-Silva, P. O. Berggren and A. Caicedo (2014). "Control of insulin secretion by cholinergic signaling in the human pancreatic islet." Diabetes **63**(8): 2714-2726.

Moreno, A. P., V. M. Berthoud, G. Pérez-Palacios and E. M. Pérez-Armendariz (2005). "Biophysical evidence that connexin-36 forms functional gap junction channels between pancreatic mouse β-cells." American Journal of Physiology - Endocrinology And Metabolism **288**(5): E948-E956.

Muraro, Mauro J., G. Dharmadhikari, D. Grün, N. Groen, T. Dielen, E. Jansen, L. van Gurp, Marten A. Engelse, F. Carlotti, Eelco J. P. de Koning and A. van Oudenaarden (2016). "A Single-Cell Transcriptome Atlas of the Human Pancreas." Cell Systems **3**(4): 385-394.e383.

Nasteska, D. and D. J. Hodson (2018). "The role of beta cell heterogeneity in islet function and insulin release." J Mol Endocrinol **61**(1): R43-r60.

Palti, Y., G. BenDavid, E. Lachov, Y. H. Mika, G. Omri and R. Schatzberger (1996). "Islets of Langerhans generate wavelike electric activity modulated by glucose concentration." Diabetes **45**(5): 595-601.

Pedersen, M. G., A. Tagliavini and J. C. Henquin (2019). "Calcium signaling and secretory granule pool dynamics underlie biphasic insulin secretion and its amplification: experiments and modeling." Am J Physiol Endocrinol Metab.

Ravier, M. A., M. Güldenagel, A. Charollais, A. Gjinovci, D. Caille, G. Söhl, C. B. Wollheim, K. Willecke, J.-C. Henquin and P. Meda (2005). "Loss of Connexin36 Channels Alters β-Cell Coupling, Islet Synchronization of Glucose-Induced Ca2+ and Insulin Oscillations, and Basal Insulin Release." Diabetes **54**(6): 1798-1807.

Rutter, G. A. and D. J. Hodson (2013). "Minireview: intraislet regulation of insulin secretion in humans." Mol Endocrinol **27**(12): 1984-1995.

Rutter, G. A. and D. J. Hodson (2014). "Beta cell connectivity in pancreatic islets: a type 2 diabetes target?" Cell Mol Life Sci.

Satin, L. S. (2000). "Localized calcium influx in pancreatic beta-cells: its significance for Ca2+-dependent insulin secretion from the islets of Langerhans." Endocrine **13**(3): 251-262.

Satin, L. S., P. C. Butler, J. Ha and A. S. Sherman (2015). "Pulsatile insulin secretion, impaired glucose tolerance and type 2 diabetes." Mol Aspects Med.

Skelin Klemen, M., J. Dolenšek, M. Slak Rupnik and A. Stožer (2017). "The Triggering Pathway to Insulin Secretion: Functional Similarities and Differences Between the Human and the Mouse Beta Cells and their Translational Relevance." Islets: 00-00.

Speier, S. and M. Rupnik (2003). "A novel approach to in situ characterization of pancreatic ß-cells." Pflügers Archiv European Journal of Physiology **446**(5): 553-558.

Stetter, O., D. Battaglia, J. Soriano and T. Geisel (2012). "Model-free reconstruction of excitatory neuronal connectivity from calcium imaging signals." PLoS Comput Biol **8**(8): e1002653.

Stožer, A., J. Dolenšek and M. S. Rupnik (2013). "Glucose-Stimulated Calcium Dynamics in Islets of Langerhans in Acute Mouse Pancreas Tissue Slices." PLoS ONE **8**(1): e54638.

Stožer, A., M. Gosak, J. Dolenšek, M. Perc, M. Marhl, M. S. Rupnik and D. Korošak (2013). "Functional Connectivity in Islets of Langerhans from Mouse Pancreas Tissue Slices." PLoS Comput Biol **9**(2): e1002923.

Westacott, M. J., N. L. Farnsworth, J. R. St Clair, G. Poffenberger, A. Heintz, N. W. Ludin, N. J. Hart, A. C. Powers and R. K. P. Benninger (2017). "Age-Dependent Decline in the Coordinated [Ca(2+)] and Insulin Secretory Dynamics in Human Pancreatic Islets." Diabetes **66**(9): 2436-2445.

Zhang, Q., J. Galvanovskis, F. Abdulkader, C. J. Partridge, S. O. Gopel, L. Eliasson and P. Rorsman (2008). "Cell coupling in mouse pancreatic beta-cells measured in intact islets of Langerhans." Philos Transact A Math Phys Eng Sci **366**(1880): 3503-3523.

Zhu, S., D. Larkin, S. Lu, C. Inouye, L. Haataja, A. Anjum, R. Kennedy, D. Castle and P. Arvan (2016). "Monitoring C-Peptide Storage and Secretion in Islet β-Cells In Vitro and In Vivo." Diabetes **65**(3): 699-709.

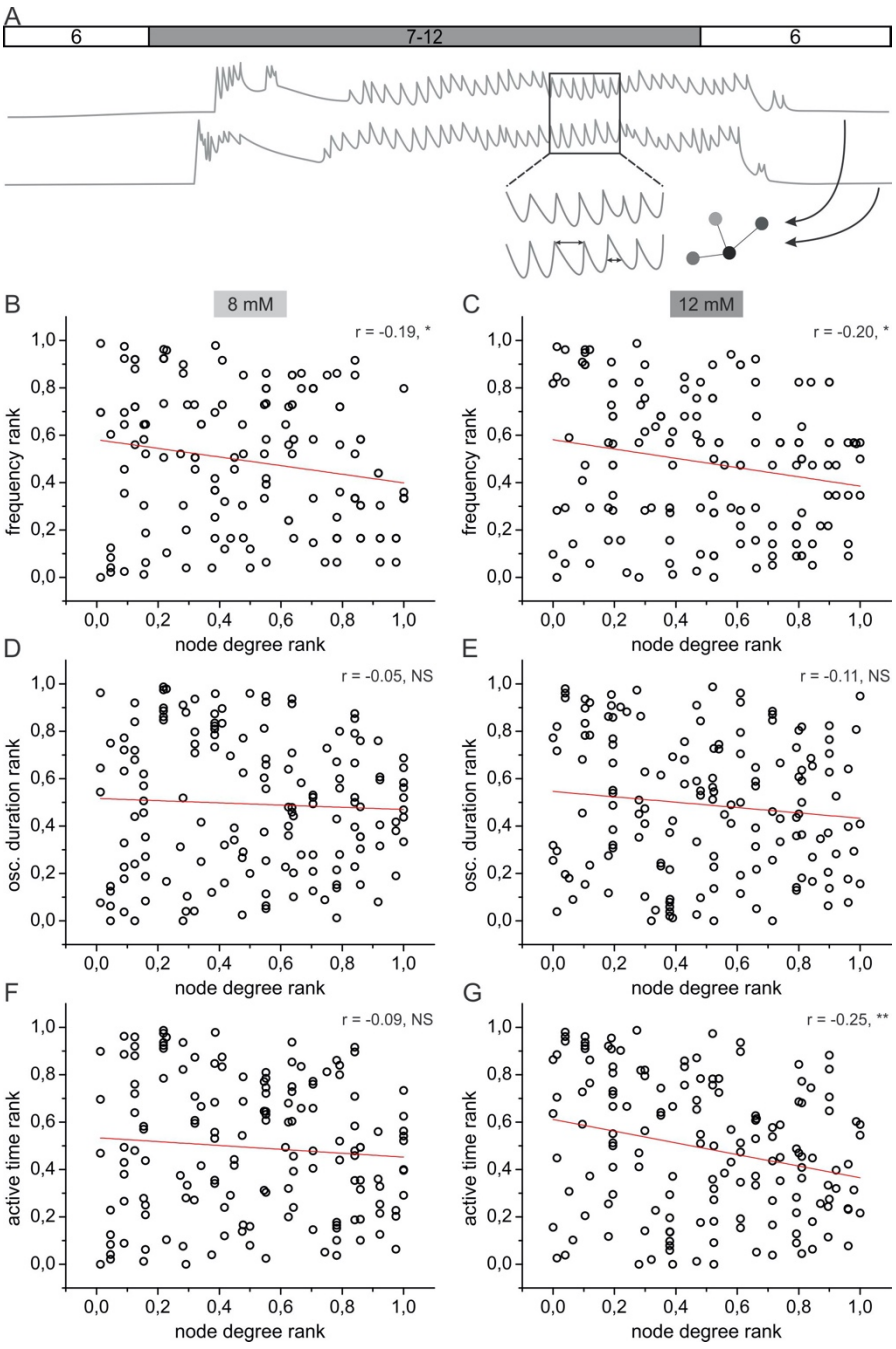


***Figure S1. Correlation between node degrees and oscillation frequency, duration, and active time during plateau phase.*** ***A*** *Schematic cartoon depicting measured parameters.* ***B-G*** *Average frequency rank (B-C), oscillation duration rank (D-E) and relative active time rank (F-G) as a function of node degree rank for 8 mM (B, D, and F) and 12 mM (C, E, and G) glucose. Results are based on 152 cells from 3 islets under 8 mM glucose and 151 cells from the islets under 12 mM glucose.*

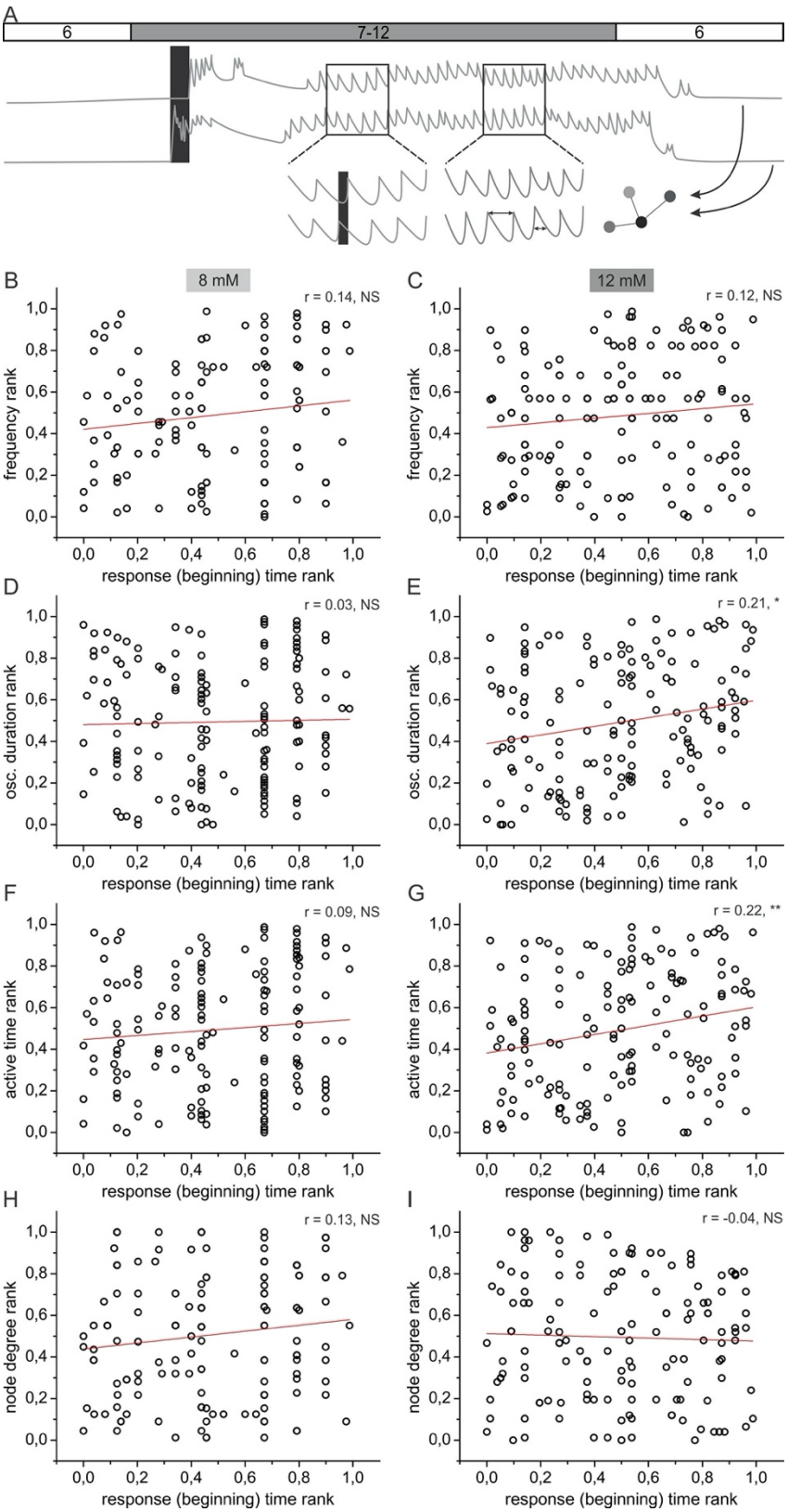


***Figure S2. Correlations between response activation of cells and plateau phase response properties. A*** *Schematic cartoon depicting measured parameters.* ***B-I*** *Response activation ranks as a function of response frequency (B-C), duration (D-E), active time (F-G), and node degree (H-I) after switching from 6 mM to 8 mM (B, D, F, and H) or 12 mM (C, E, G, and I) glucose. Results are based on 152 cells from 3 islets under 8 mM glucose and 151 cells from the islets under 12 mM glucose.*

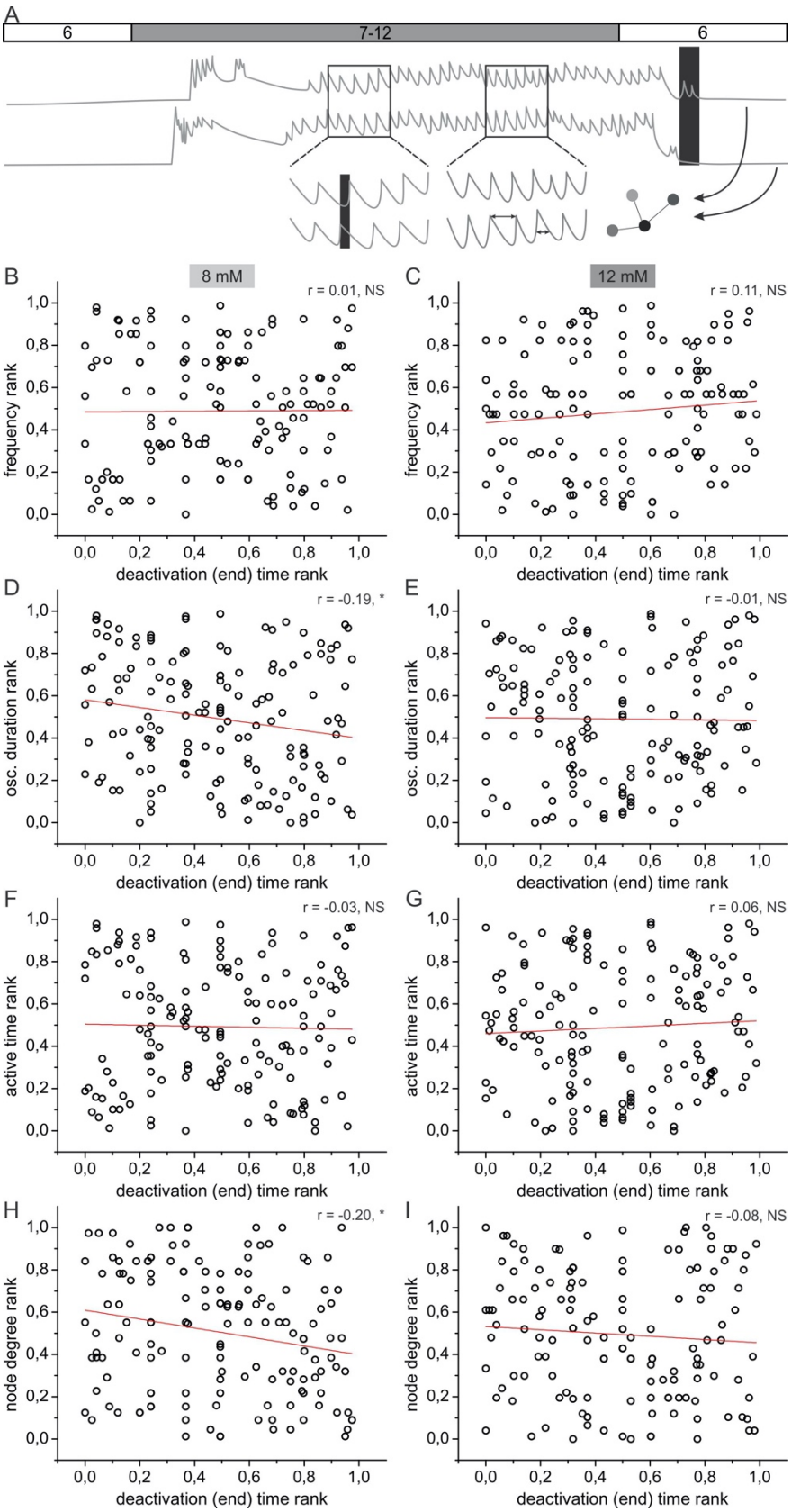


**Figure S3.** ***Correlations between response deactivation of cells and plateau phase response properties. A*** *Schematic cartoon depicting measured parameters.* ***B-I*** *Response deactivation ranks as a function of response frequency (B-C), duration (D-E), active time (F-G), and node degree (H-I) after switching from 6 mM to 8 mM (B, D, F, and H) or 12 mM (C, E, G, and I) glucose. Results are based on 152 cells from 3 islets under 8 mM glucose and 151 cells from the islets under 12 mM glucose.*